

Dynamic Nuclear Polarization in Silicon Microparticles

A. E. Dementyev^{1*}, D. G. Cory², and C. Ramanathan²

¹*Francis Bitter Magnet Laboratory, Massachusetts Institute of Technology, Cambridge, MA 02139, USA*

²*Department of Nuclear Science and Engineering,
Massachusetts Institute of Technology, Cambridge, MA 02139, USA*

(Dated: October 28, 2018)

We report record high ^{29}Si spin polarization obtained using dynamic nuclear polarization in microcrystalline silicon powder. Unpaired electrons in this silicon powder are due to dangling bonds in the amorphous region of this intrinsically heterogeneous sample. ^{29}Si nuclei in the amorphous region become polarized by forced electron-nuclear spin flips driven by off-resonant microwave radiation while nuclei in the crystalline region are polarized by spin diffusion across crystalline boundaries. Hyperpolarized silicon microparticles have long T_1 relaxation times and could be used as tracers for magnetic resonance imaging.

PACS numbers: 76.70.Fz, 81.07.Bc, 03.67.Lx, 82.56.-b

Crystalline and amorphous silicon are both of great technological importance. Single-crystal silicon is a workhorse of the electronic industry while amorphous silicon is widely used for photovoltaic devices. Recently, several promising silicon-based architectures have been proposed for quantum computing [1, 2, 3]. The long coherence times of ^{29}Si and ^{31}P nuclear spins in lightly doped silicon crystals make them attractive candidates for quantum bits (qubits) [4, 5]. One of the major limitations of using nuclear spins as qubits is the highly mixed state of the nuclear spin system at thermal equilibrium [6, 7, 8]. Several methods can be used to hyperpolarize nuclear spin systems. For instance, optical pumping techniques have been very successful in studies of electron spin physics in gallium arsenide quantum wells and quantum dots [9, 10] but so far have produced comparatively low nuclear spin polarization in silicon [11, 12, 13]. Microwave induced dynamic nuclear polarization (DNP) is a powerful technique, where an enhancement of several orders of magnitude of the nuclear spin polarization can be generated by microwave irradiation of paramagnetic centers coupled to the nuclear spin system through the hyperfine interaction [14, 15]. Since the discovery of DNP in 1953 [16, 17], there have been several reports of DNP in silicon [18, 19, 20], but all of them were done either at high temperatures or low magnetic fields limiting the ^{29}Si spin polarization to a few percent. It is imperative for the emerging fields of spintronics [21] and nanotechnology to develop methods to achieve high ^{29}Si spin polarization in both bulk and nanoscale samples.

Here, we report the first DNP experiments in undoped silicon microparticles. The amorphous region of these particles has a very high concentration of structural de-

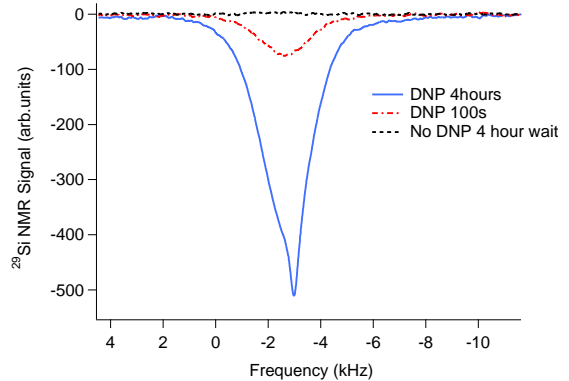


FIG. 1: ^{29}Si NMR spectra acquired at 1.4K for different microwave irradiation times in $B=2.35\text{T}$ ($f_0=19.89\text{MHz}$). The spectrum acquired without the microwave irradiation is shown using the dashed line.

fects - dangling bonds [22]. ^{29}Si nuclei in this region are polarized by microwave irradiation of the hyperfine coupled electron-nuclear spin system. The density of paramagnetic impurities in the crystalline cores is low which results in the long nuclear relaxation times. Nuclei in those regions are polarized by nuclear spin diffusion [23] across crystalline boundaries. Several orders of magnitude enhancement of the NMR signal combined with the long T_1 relaxation time makes this a valuable technique for hyperpolarizing silicon nanoparticles, with potential applications in medical imaging [24, 25] and NMR studies of nanoscale systems (e.g. silicon nanowires).

Our sample is a polycrystalline powder obtained from Alfa Aesar. It is 99.999% pure with particle sizes distributed between 1 and 5 μm . According to X-ray diffraction analysis of this sample 80% of the sample is amorphous while 20% is crystalline and individual crystallites are larger than 200nm. Our DNP experiments were

*Author to whom correspondence should be addressed. Electronic address: anatolyd@physics.harvard.edu

performed at 1.4 K in a 2.35 T superconducting NMR magnet. An Oxford NMR Spectrostat was operated in single-shot mode to cool the sample down to 1.4 K. The microwave source was a 90 mW Gunn diode source (Millitech). The NMR spectrometer used was a Bruker Avance system with a home-built probe, containing a horn antenna for the microwave irradiation of the sample, and a solenoidal NMR rf coil, that were in direct contact with pumped liquid helium. Details of a similar probe design have been described elsewhere[26].

Figure 1 shows the ^{29}Si NMR spectra acquired without and with microwave irradiation at 66.25 GHz for different irradiation times. For short irradiation times the NMR spectrum is inhomogeneously broadened with a 2 kHz linewidth (full width at half of a maximum height) due to the distribution of distances between nuclear and electron spins in the amorphous region. The sharp feature in the spectrum is due to nuclei in the crystalline cores and appears for microwave irradiation times longer than an hour. The 300 Hz linewidth of this feature is consistent with previous NMR measurements on silicon crystalline powder samples [27] and can be explained by a combination of dipole-dipole interaction between ^{29}Si nuclei arranged in the crystalline lattice and magnetic susceptibility broadening. The average DNP enhancement of the nuclear polarization for the amorphous phase inferred from Fig.1 is 150, corresponding to a ^{29}Si polarization of 5%. We believe this to be the highest ^{29}Si polarization yet achieved. Nuclear polarization of the crystalline region after 4 h of DNP is found to be $\sim 2\%$. This estimate comes from the ratio of the integrated NMR signals from amorphous and crystalline regions and takes into account that crystalline region is only 20% of the sample.

We performed ESR studies to characterize the nature of the paramagnetic centers in our sample. The g-factor value $g = 2.006$, obtained from our ESR spectra is consistent with earlier measurements in amorphous silicon [22] that identified the defects as dangling bonds. Figure 2(a) shows the low temperature ESR spectrum which was acquired in the rapid-passage regime with the spectrometer tuned to dispersive response. The electron spin T_1 relaxation time was estimated to be approximately 30 μs using the rapid-passage phase method [28].

Figure 2(b) shows the dependence of the NMR signal amplitude on the microwave frequency for a microwave irradiation time of 200 s acquired at 2.35T and 1.4K. It is characteristic of the DNP thermal mixing mechanism. This is a typical DNP mechanism in insulators with a high concentration of paramagnetic impurities at low temperatures [14, 15, 29]. Microwave irradiation just below the ESR central frequency cools the electron spin dipolar reservoir while microwave irradiation just above the ESR central frequency creates a negative temperature for the electron spin dipolar reservoir. Since the ESR linewidth is larger than the nuclear Larmor frequency, the electron spin flip-flop interaction mediated

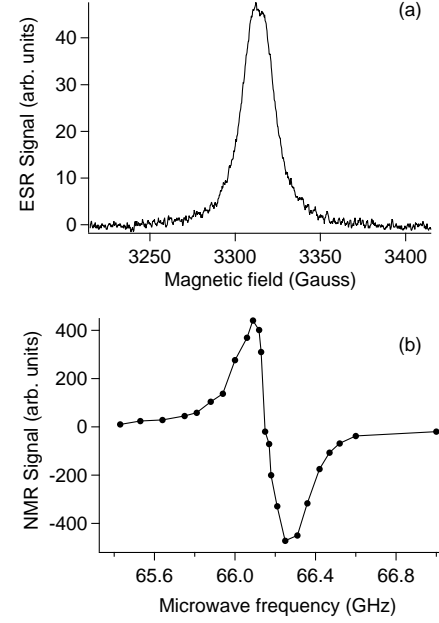


FIG. 2: (a) The ESR spectrum acquired at 3.6 K and 9.27 GHz. (b) The dependence of the NMR signal amplitude on microwave frequency acquired at 2.35T and 1.4K for a microwave irradiation time of 200 s.

by nuclear spin flips equalizes the electron spin dipolar temperature with the nuclear spin temperature.

The microwave irradiation time dependence of the NMR signal amplitude is shown in Fig. 3(a). There are two distinct time scales. Within the first hour ^{29}Si nuclei in the amorphous region are hyperpolarized through the thermal mixing mechanism. Beyond the first hour the NMR signal continues to increase because of spin diffusion into the crystalline cores. There is still an increase of the signal for times after 4 h. This is consistent with very slow spin diffusion in the network of naturally abundant ^{29}Si spins mediated by XY terms of the dipolar interaction:

$$\frac{\mathcal{H}_d}{\hbar} = \sum_{j>i} a_{ij} \left\{ I_{z_i} I_{z_j} - \frac{1}{2} (I_{x_i} I_{x_j} + I_{y_i} I_{y_j}) \right\}, \quad (1)$$

where $a_{ij} = \frac{(\gamma^{29})^2 \hbar}{r_{ij}^3} [1 - 3 \cos^2 \theta_{ij}]$ (γ^{29} is the gyromagnetic ratio for ^{29}Si). The vector between spins i and j , \vec{r}_{ij} , satisfies $\vec{r}_{ij} \cdot \hat{z} = r_{ij} \cos \theta_{ij}$. Magnetization transport is described by the diffusion equation:

$$\frac{\partial M}{\partial t} = D \Delta M \quad (2)$$

where $D \cong \frac{b^2}{50T_2}$ is the diffusion constant [23], T_2 is the nuclear transverse relaxation time and b is the average distance between neighboring ^{29}Si nuclei. Assuming in our case $T_2 \approx 5.6\text{ms}$ [27] and $b \approx 0.55n^{-1/3} \approx 0.41\text{nm}$

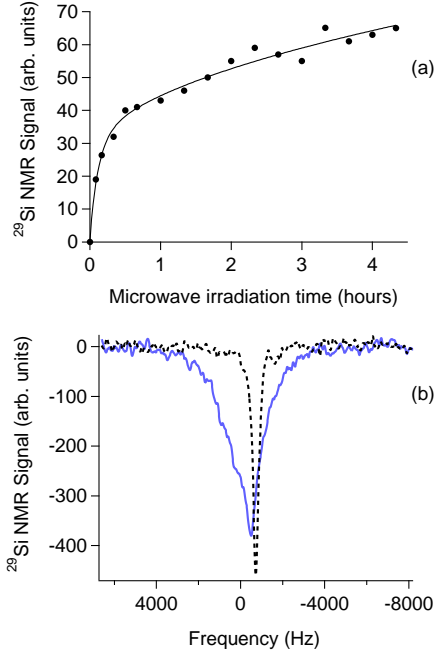


FIG. 3: (a) The dependence of the NMR signal amplitude on microwave irradiation time. The solid line is to guide the eye. (b) Two ^{29}Si NMR spectra, the solid line is the spectrum acquired after 4 h of DNP at 1.4K with a 5° tipping pulse and the dashed line is the spectrum acquired after the microwave irradiation was turned off and the sample was warmed up to 240K (a 90° tipping pulse was used).

[30], where n is the density of ^{29}Si nuclei, we estimate $D \cong 6 \times 10^{-15} \text{ cm}^2/\text{s}$.

Once the nuclear polarization builds up inside the crystalline cores of the particles it can be stored for a time on the order of the nuclear T_1 relaxation time. For example, Fig 3(b) shows two ^{29}Si NMR spectra, one (solid line) was acquired after 4 h of DNP at 1.4K with a short (5°) NMR pulse, while the other one (dashed line) was acquired after the microwave irradiation was turned off and the sample was slowly warmed up to 240K. The broad line from the amorphous phase quickly disappeared due to the fast relaxation rate of the amorphous domain and only the narrow component from the crystalline cores survived after an hour long warming up procedure. The resulted ^{29}Si polarization is about 3000 times higher than the equilibrium polarization at 240K.

In order to estimate the ^{29}Si nuclear T_1 in the crystalline part of the sample, we prepared nuclear spin polarization by DNP at 1.4K for 5 h, allowing for nuclear spin diffusion to penetrate inside the crystalline cores. Afterwards, the microwave radiation was turned off and the cryostat was warmed up to 4.2K to enable the continuous flow operation. Figure 4(a) shows the decay of the NMR signal amplitude from the crystalline cores together with a simulation (solid line) using the diffusion equation (Eq. 2) for a spherical particle with a radius of

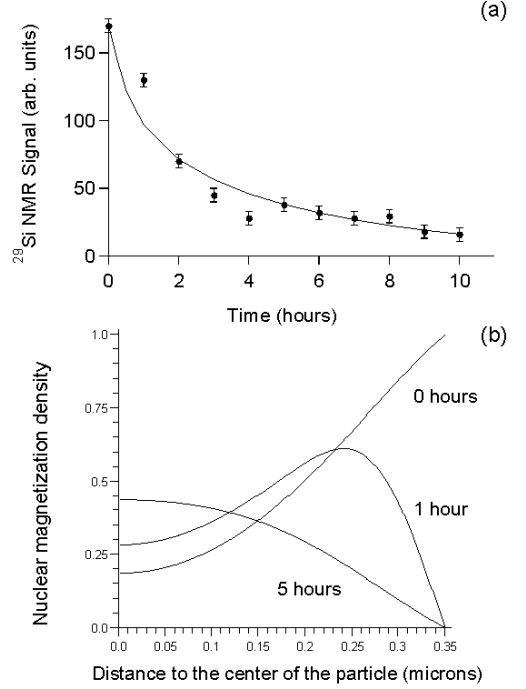


FIG. 4: (a) The decay of the NMR signal from crystalline silicon after DNP for 5 h at 1.4K. We used 15° NMR pulses to monitor the signal decay. The solid line is the calculation of the decay due to the spin diffusion of nuclear polarization to the surface. (b) Simulated nuclear spin magnetization density profiles in a spherical particle with a radius of 350nm corresponding to different time points in (a): right after DNP (labeled 0 hours), 1 hour and 5 hours after DNP.

350nm. In combination with the large initial polarization, it is the long T_1 observed here that underlies the potential use of these particles as tracers.

In the simulation we set the magnetization density on the surface of the particle to a finite value for the 5 h DNP period and to a zero right afterwards. The nuclear spin magnetization density profiles obtained using this simulation are shown in Fig. 4(b). The agreement between the experiment and the simulation is satisfactory given the simplicity of the model. The decay of the spin magnetization in this model depends on the particle size and the nuclear spin diffusion coefficient. Although the decay is nonexponential, we calculate the nuclear spin-lattice relaxation time T_1 as the time when magnetization decays to $1/e$ of the initial value. It scales as $T_1 \propto \frac{R^2}{D}$, where R is the radius of a particle. There is an interplay between the initial magnetization and the T_1 on one side, and the isotopic abundance of ^{29}Si on the other. High ^{29}Si concentration leads to a larger initial magnetization but also to a larger nuclear spin diffusion coefficient and thus a shorter T_1 . The result is that isotopic enrichment reduces the storage time. Figure 5 shows simulations of the ^{29}Si magnetization decay due to spin diffusion and instantaneous relaxation at the surface for different parti-

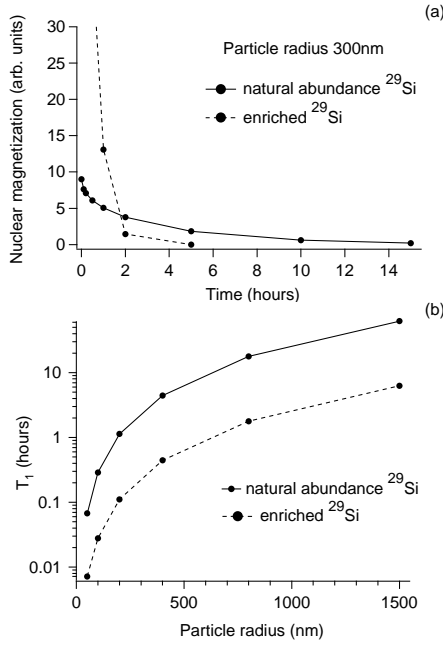


FIG. 5: (a) Simulations of the ^{29}Si magnetization decay due to spin diffusion and instantaneous relaxation at the surface for particles with 300nm radius. (b) Simulated T_1 relaxation time as a function of the particle size. Solid line is for the naturally abundant ^{29}Si and dashed line is for the ^{29}Si enriched sample.

cle sizes and for naturally abundant (4.67%) and enriched (100%) ^{29}Si . The ratio of spin diffusion coefficients for enriched and naturally abundant ^{29}Si is about 10 [31]. Although the initial magnetization density is 21.4 times larger for enriched silicon, the magnetization decay is also much faster due to faster diffusion and there is always a crossing between the two curves at long times.

In summary, we have extended previous DNP experiments in silicon to lower temperature and higher magnetic field and have achieved record high ^{29}Si spin polarization in silicon microparticles. This technique might also be used for polarizing nuclei in thin films of crystalline silicon if a layer of amorphous silicon is created on top (e.g., by ion implantation). Nuclear spin diffusion in ^{29}Si abundant crystals is significantly faster which will make it possible to polarize thicker films. The decay of nuclear spin polarization in the crystalline part of the sample is due to nuclear spin diffusion to the surface and subsequent relaxation by paramagnetic impurities. The use of hyperpolarized nanoparticles as tracers depends on both the size and time scales of interest in a given application. While moderately sized particles can retain their polarization for a relatively long time, the relaxation becomes very fast for the smallest nanoparticles.

A.E.D thanks C.M. Marcus, R.L. Walsworth, S.E. Barrett, and J. Baugh for helpful discussions, and S.A. Speakman for the X-ray diffraction analysis of our sample. This work was supported in part by the National Se-

curity Agency (NSA) under Army Research Office (ARO) contract number DAAD190310125, the NSF and DARPA DSO.

-
- [1] B.E. Kane, *Nature* **393**, 133 (1998); *Fortschr. Phys.* **48**, 1023 (2000).
 - [2] R. Vrijen, E. Yablonovitch, K. Wang, H.W. Jiang, A. Balandin, V. Roychowdhury, T. Mor, and D. DiVincenzo, *Phys. Rev. A* **62**, 012306 (2000).
 - [3] T.D. Ladd, J.R. Goldman, F. Yamaguchi, Y. Yamamoto, E. Abe, and K.M. Itoh, *Phys. Rev. Lett.* **89**, 017901 (2002); K.M. Itoh, *Solid State Commun.* **133**, 747 (2005).
 - [4] A. Abragam, *The Principles of Nuclear Magnetism* (Clarendon Press, Oxford, 1961).
 - [5] G. Feher, E.A. Gere, *Phys. Rev.* **114**, 1245 (1959).
 - [6] D.G. Cory, A.F. Fahmy, T.F. Havel, *Proc. Natl. Acad. Sci. U.S.A.* **94**, 1634 (1997).
 - [7] N.A. Gershenfeld and I.L. Chuang, *Science* **275**, 350 (1997).
 - [8] W.S. Warren, *Science* **277**, 1688 (1997).
 - [9] S.E. Barrett, G. Dabbagh, L.N. Pfeiffer, K.W. West, R. Tycko, *Phys. Rev. Lett.* **74**, 5112 (1995); R. Tycko, S.E. Barrett, G. Dabbagh, L.N. Pfeiffer, K.W. West, *Science* **268**, 1460 (1995).
 - [10] A.S. Bracker *et al.*, *Phys. Rev. Lett.* **94**, 047402 (2005).
 - [11] G. Lampel, *Phys. Rev. Lett.* **20**, 491 (1968).
 - [12] N.T. Bagraev and L.S. Vlasenko, *Sov. Phys. Solid State* **24**, 1974 (1982).
 - [13] A.S. Verhulst, I.G. Rau, Y. Yamamoto, K.M. Itoh, *Phys. Rev. B* **71**, 235206 (2005).
 - [14] A. Abragam and M. Goldman, *Nuclear Magnetism: Order and Disorder* (Clarendon Press, Oxford, 1982).
 - [15] V. Weis and R.G. Griffin, *Solid State NMR* **29**, 66 (2006).
 - [16] A.W. Overhauser, *Phys. Rev.* **92**, 411 (1953).
 - [17] T.R. Carver and C.P. Slichter, *Phys. Rev.* **92**, 212 (1953).
 - [18] A. Abragam, J. Combrisson, I. Solomon, *Compt. Rend.* **246**, 1035 (1958).
 - [19] H. Lock, R.A. Wind, G.E. Maciel, N. Zumbulyadis, *Solid State Commun.* **64**, 41 (1987).
 - [20] A. Henstra, P. Dirksen, W.T. Wenckebach, *Phys. Lett. A* **134**, 134 (1988).
 - [21] S.A. Wolfe *et al.*, *Science* **294**, 1488 (2001).
 - [22] M.H. Brodsky and R.S. Title, *Phys. Rev. Lett.* **23**, 581 (1969).
 - [23] N. Bloembergen, *Physica* **15**, 386 (1949).
 - [24] C.M. Marcus (private communication).
 - [25] P. Sharma, S. Brown, G. Walter, S. Santra, B. Moudgil, *Adv. Colloid Interface Sci.* **123**, 471 (2006).
 - [26] H. Cho, J. Baugh, C.A. Ryan, D.G. Cory, C. Ramanathan, *J. Magn. Reson.* **187**, 242 (2007).
 - [27] A.E. Dementyev, D. Li, K. MacLean, S.E. Barrett, *Phys. Rev. B* **68**, 153302 (2003).
 - [28] P.R. Cullis and J.R. Marko, *Phys. Rev. B* **11**, 4184 (1975).
 - [29] C.T. Farrar, D.A. Hall, G.J. Gerfen, S.J. Inati, R.G. Griffin, *J. Chem. Phys.* **114**, 4922 (2001).
 - [30] M.J.R. Hoch and E.C. Reynhardt, *Phys. Rev. B* **37**, 9222 (1988).
 - [31] I.M. Nolden and R.J. Silbey, *Phys. Rev. B* **54**, 381 (1996).